



## Biaxial fatigue tests and crack paths for AISI 304L stainless steel

V. Chaves, C. Madrigal, A. Navarro

*University of Sevilla, Departamento de Ingeniería Mecánica y Fabricación. Escuela Técnica Superior de Ingeniería.  
Avenida Camino de los Descubrimientos s/n. 41092. Sevilla, Spain.*

*chavesrv@us.es*

**ABSTRACT.** AISI 304L stainless steel specimens have been tested in fatigue. The tests were axial, torsional and in-phase biaxial, all of them under load control and  $R=-1$ . The S-N curves were built following the ASTM E739 standard and the method of maximum likelihood proposed by Bettinelli. The fatigue limits of the biaxial tests were represented in axes  $\sigma$ - $\tau$ . The elliptical quadrant, appropriate for ductile materials, and the elliptical arc, appropriate for fragile materials, were included in the graph. The experimental values were better fitted with an elliptical quadrant, despite the ratio between the pure torsion and tension fatigue limits,  $\tau_{FL}/\sigma_{FL}$ , is 0.91, close to 1, which is a typical value for fragile materials. The crack direction along the surface has been analyzed by using a microscope, with especial attention to the crack initiation zones. The crack direction during the Stage I has been compared with theoretical models.

**KEYWORDS.** Multiaxial fatigue; S-N curve; Crack direction; Stage I.

### INTRODUCTION

The crack direction in the initiation zone (Stage I) in planar specimens of ductile materials under fatigue is widely assumed to coincide with the maximum tangential stress direction (Mode II), and so is that for fragile materials with the maximum normal stress direction (Mode I). A material is considered to be ductile under fatigue if its torsional-to-tensile fatigue limit ratio ( $\tau_{FL}/\sigma_{FL}$ ) is close to 0.5 and fragile if the ratio is near-unity. It is unclear whether a material with an intermediate ratio will behave as ductile or fragile and whether any Stage I crack growth directions exist in between Modes I and II. In this work, we explored these possibilities.

This paper reports the experimental results for crack growth in the initiation zone in cylindrical specimens of AISI 304L stainless steel as obtained in several series of tests under controlled uniaxial and biaxial loads. The experimental results were used to construct the S-N curves and the biaxial fatigue curve for the material. Also, the direction of crack growth on the specimen surface for tests that lasted a large number of cycles (high cycle fatigue) was examined, focusing on the crack initiation zone, and compared with the predictions of various theoretical models.

### MATERIAL AND SPECIMENS

The specimens used were round bars of commercially available austenitic stainless steel (AISI 304L). The chemical composition of the steel, in wt%, was as follows: 0.021 C, 0.029 P, 0.024 S, 0.34 Si, 1.48 Mn, 18.23 Cr, 8.15 Ni, 0.21 Mo, 0.080 N and 0.39 Cu. Microstructurally, the material consisted of austenite grains of roughly equiaxial



geometry, in addition to a small amount of delta ferrite bands. The mean size of the austenite grains was  $80\ \mu\text{m}$  (see Fig. 1).

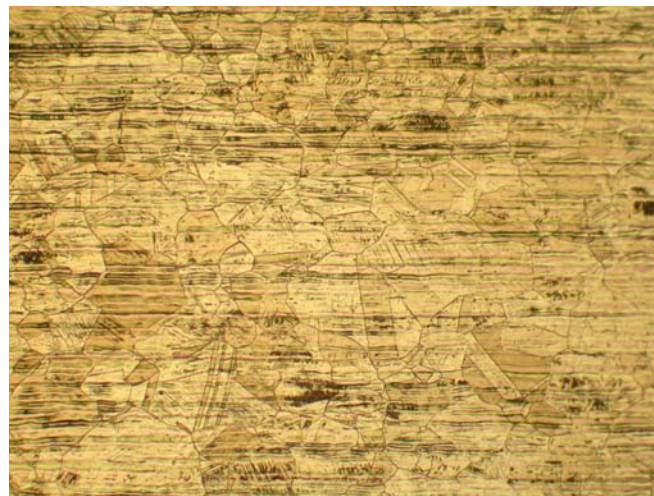


Figure 1: Microstructure of the stainless steel AISI 304L.

The mechanical properties of the steel as determined from 5 tensile tests were as follows: tensile strength ( $\sigma_{\text{UTS}}$ ) = 654 MPa, yield stress 0.2% ( $\sigma_y$ ) = 467 MPa and elongation = 56%.

The material was subjected to various biaxial fatigue laboratory tests including tensile, torsional and in-phase tensile-torsional, all at  $R = -1$ . Tests were conducted on specimens of cylindrical cross-section having a central diameter of 12.5 mm (see Fig. 2). All specimens were carefully polished to an average surface roughness ( $R_a$ ) not exceeding  $0.1\ \mu\text{m}$ . Also, all tests were performed on a biaxial fatigue hydraulic machine under controlled loading conditions, using a sine wave and a frequency of 6–8 Hz. Each test was finished when the crack grew several millimetres long (in some cases the specimen broke completely) or a number of  $3.5 \times 10^6$  cycles (run-outs) was reached.

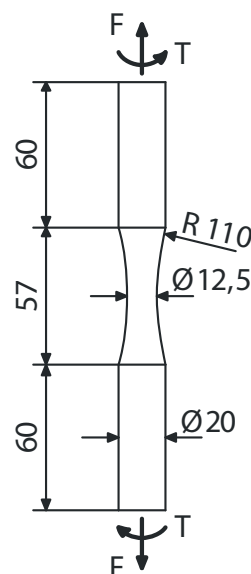


Figure 2: Geometry of the cylindrical specimens tested in biaxial fatigue (in mm).

## S-N CURVES

The results of the above-described tests were used to construct  $S-N$  curves in accordance with ASTM E 739-91 (2004) [1]. Based on this standard, the variables stress and number of cycles to failure can be approximated by a linear logarithmic relationship, excluding run-outs. The fatigue limits were calculated using the maximum



likelihood method proposed by Betinelli [2]. This procedure, which uses both the failures and the run-outs, is an effective alternative to classical choices such as the staircase method and requires less experimental testing. The two straight lines were plotted in a single graph in order to obtain predictions throughout the entire life.

Fig. 3 and 4 show in a semi-logarithmic graph the experimental  $S-N$  curves for the monoaxial and biaxial tests, respectively. As can be seen, the curves were extremely horizontal. In fact, the difference between withstanding a few thousands of cycles only and not breaking was a few megapascals. This material exhibits a dual behaviour: either it exhibits a very short lifetime or does not break at all. It was therefore impossible to detect breaking points after around a million cycles since any specimens reaching those lifetimes failed to break beyond that point. Also, having such a horizontal  $S-N$  curve had the advantage that fatigue limit calculations were subject to very little uncertainty.

The tensile-compressive fatigue limit ( $R = -1$ ) for the material as determined in cylindrical specimens and expressed in stress amplitude was  $\sigma_{FL} = 316$  MPa and its torsional counterpart  $\tau_{FL} = 288$  MPa.

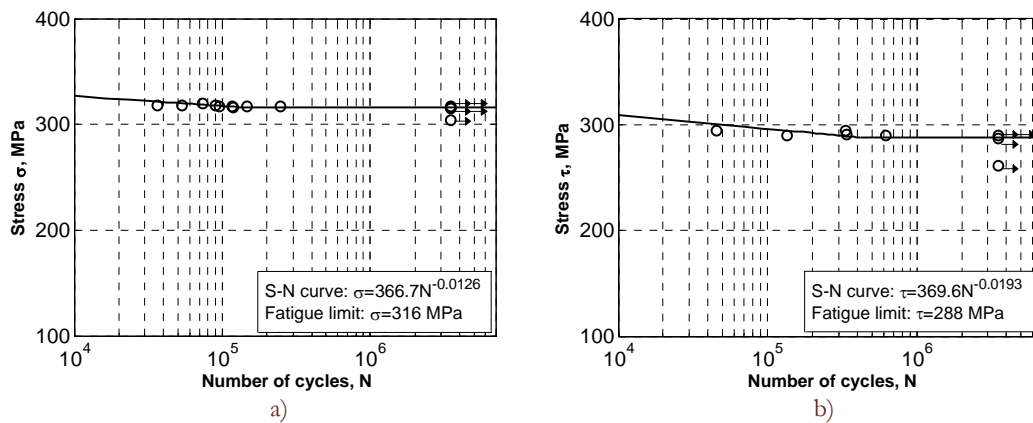


Figure 3: S-N curves for the monoaxial tests ( $R=-1$ ): a) push-pull, b) torsion.

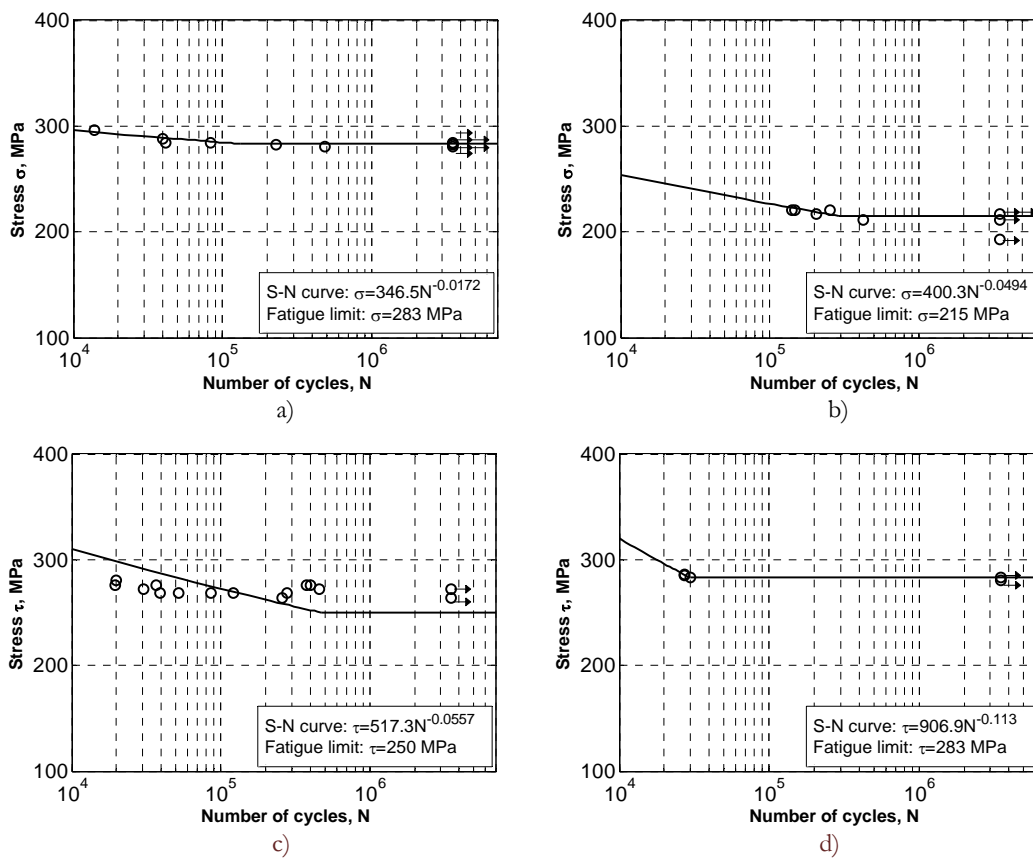


Figure 4: S-N curves for the biaxial tests ( $R=-1$ ): a)  $0.5\sigma = \tau$ , b)  $\sigma = \tau$ , c)  $2\sigma = \tau$ , d)  $4\sigma = \tau$ .



## BIAXIAL FATIGUE CURVE

The fatigue limits obtained from biaxial loading tests on cylindrical specimens can be used to construct  $\sigma$ - $\tau$  plots. As can be seen from Fig. 5, our experimental values fitted an elliptical quadrant better than an elliptical arc. Based on experimental results of Gough et al. [3], fragile materials in fatigue are optimally approximated by an arc and ductile materials by a quadrant. AISI 304L steel has a near-unity  $\sigma_{FL}/\tau_{FL}$  ratio ( $288/316 = 0.91$ ); therefore, it behaves as a fragile material in fatigue. Then, the present experimental results contradict experimental results of the previous authors for materials exhibiting a fragile behaviour under fatigue. But, certainly, the results of Gough et al. corresponded to cast irons alone.

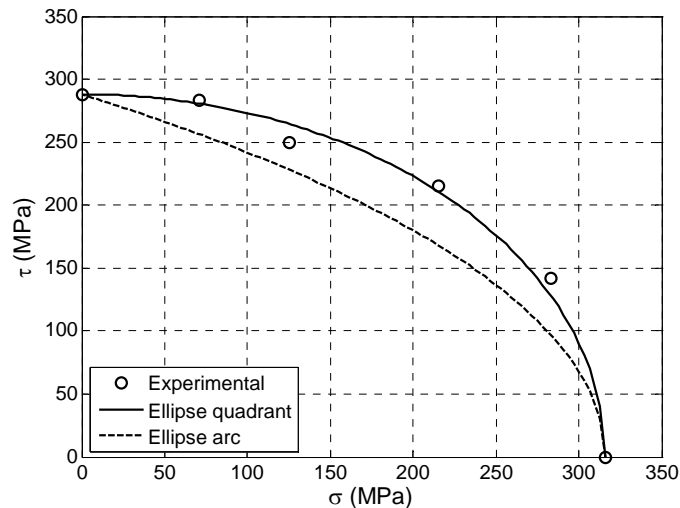


Figure 5: Experimental fatigue limits for the biaxial tests.

## CRACK DIRECTION DURING STAGE I

This section deals with crack direction across the first few grains (Stage I) as determined experimentally or predicted with various models. The X axis ran across the specimen and the Y axis along it (see Fig. 6). Determinations involved examining the crack at the specimen outer surface and measuring the angle, called  $\alpha$ , from the X axis. A second angle, named  $\theta$ , which is the angle that forms the crack with the direction that is normal to the first principal stress ( $\sigma_1$  direction) is defined for the comparison with the models.

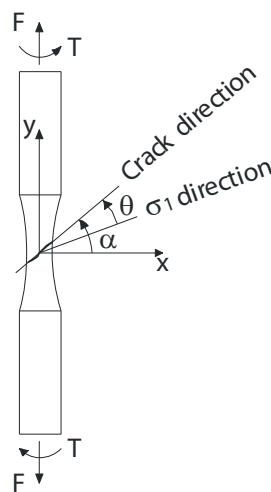


Figure 6: Axes and angles for the study of the crack direction.



### Experimental results

The experimental procedure was as follows: once the specimen broke completely or partly, a light microscope was used to photograph the surface containing the whole crack. With cylindrical specimens, this entails taking a large number of photographs and carefully assembling them with imaging software. The next step is examining the fracture surface. Incompletely broken specimens are previously subjected to tensile stress until they break into two pieces; then, one of the pieces is examined under a light microscope to locate the origin of the fatigue crack, which will coincide with the merging point of “river lines”. The crack starts in a small zone of the specimen outer surface. Some specimens develop several cracks at once but, invariably, one eventually prevails or all merge into a single, larger crack. Some crack initiation zones are additionally examined under an electronic microscope. In any case, once the small zone where the crack starts is located in the photographs, the angle between the crack and the  $X$  axis in the specimen is measured.

Below is described the application of the above-described procedure to a cylindrical specimen under axial loading. The specimen was applied a cyclic load from  $-317$  to  $317$  MPa, which caused it to break into two pieces after 145 850 cycles (see Fig. 7). As can clearly be seen in the fracture surface picture, there was a smoother, fatigue zone and a rougher rapid fracture zone. The fatigue zone exhibited several lines radiating from the fatigue initiation zone, which fell on the specimen boundary (i.e., on the specimen outer surface) and was about  $750\ \mu\text{m}$  in size. The bottom figure shows a magnified view of the crack on the outer surface and the location of the initiation zone. The angle between the crack at the initiation zone and the  $X$  axis was  $\alpha = 12^\circ$  and the zone was about 10 grains in size (i.e., at Stage I of crack growth).

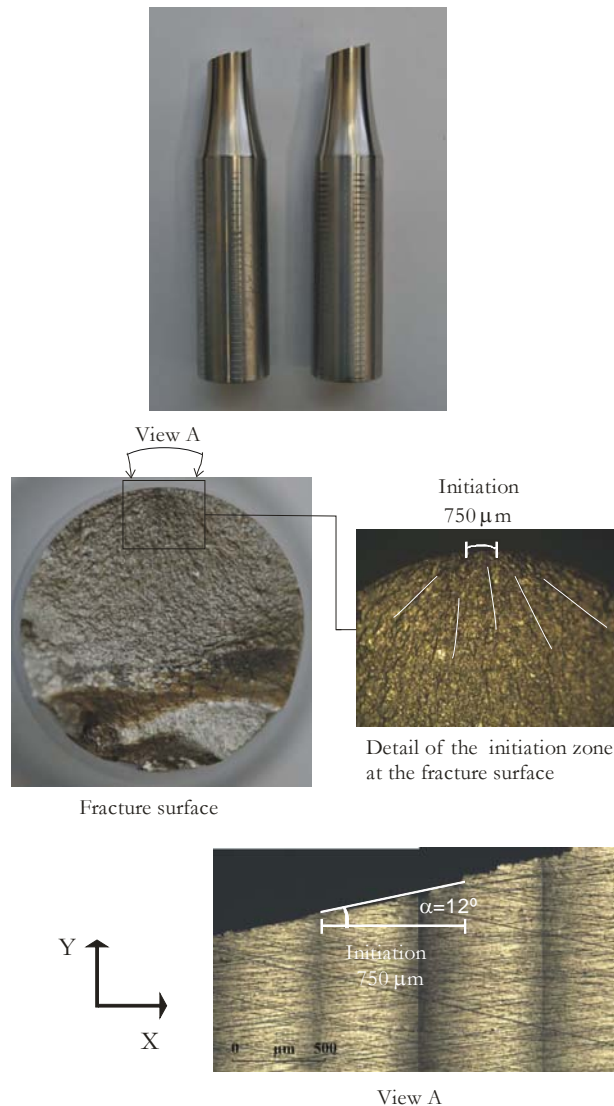


Figure 7: Broken specimen subjected to axial loading ( $R=-1$ ),  $N=145850$  cycles. Details of the fracture surface and the crack angle  $\alpha$  during the Stage I.

Fig. 8 shows a specimen under in-phase biaxial loading, the photographic montage of the crack and a magnified view of the crack angle at Stage I. The normal stress applied was twice the maximum tangential stress at the surface (i.e.,  $2\sigma = \tau$ ,  $R = -1$ ). The test lasted 398,576 cycles, during which the crack grew 17 mm long (i.e., roughly one-half the specimen perimeter), but the specimen failed to break completely. Usually, tests involving torsional loading are stopped before the specimen breaks completely in order to avoid the need for too wide a turn of the testing machine and facilitate monitoring of the crack direction and initiation zone. In addition, finishing tests before the specimen breaks prevents substantial deterioration of the fracture surface by effect of strong friction between the crack sides. As experimentally confirmed, a crack several millimetres long only requires about 100 further cycles—an insignificant number relative to a typical lifetime—for the specimen to break. Therefore, both situations are identified with fracture.

Fig. 8 also shows the fracture surface and the location of the crack initiation zone, which was 1450  $\mu\text{m}$  in size on the outer surface, as well as the angle between the Stage I crack and the X axis ( $\alpha = 37^\circ$ ). As can be seen, the crack was tilted in this zone but virtually horizontal in the crack propagation zone (Stage II). The latter was subject to heavy friction under torsion, hence its much darker colour.

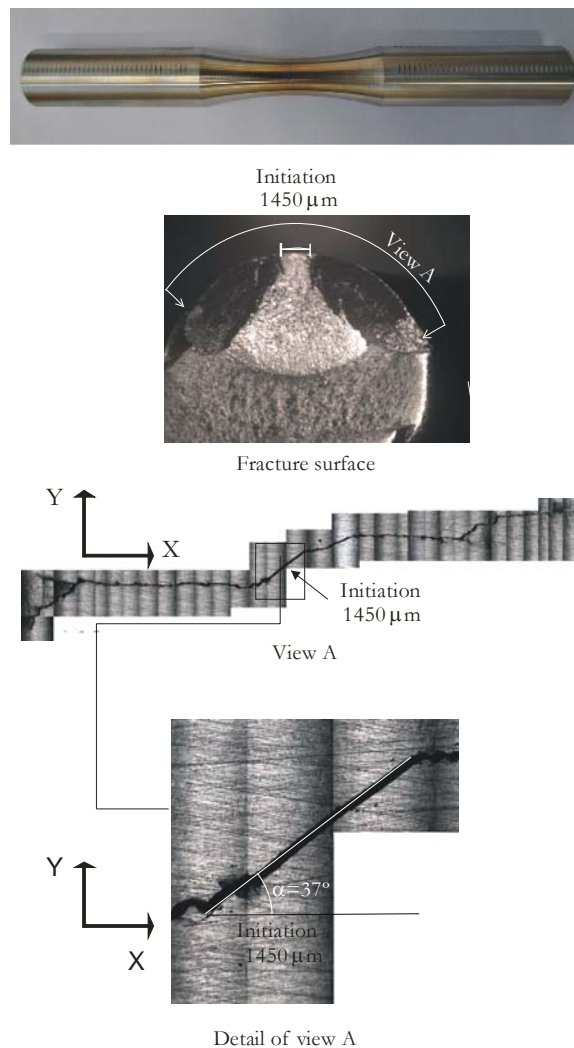


Figure 8: Broken specimen subjected to in-phase biaxial loading  $2\sigma = \tau$  ( $R=-1$ ),  $N=398576$  cycles. Details of the fracture surface and the crack angle  $\alpha$  during the Stage I.

### Model-based predictions

Recently, Chaves et al. [4] developed a method for predicting the growth direction in the initiation zone of a crack under high cycle fatigue. The method is based on the microstructural model of Navarro et al. [5] for the fatigue limit under in-phase biaxial loads. Predictions are made from two properties of the material, namely: the axial fatigue limit ( $\sigma_{FL}$ ) and the



torsional fatigue limit ( $\tau_{FL}$ ). The model calculates the angle  $\theta$  between the crack initial direction and the normal to the maximum principal stress:

$$\theta = \frac{1}{2} \arccos \left( \frac{2 - (\sigma_{FL} / \tau_{FL})}{(\sigma_{FL} / \tau_{FL})} \right) \tag{1}$$

Based on the above-described experimental  $S-N$  curves,  $\sigma_{FL}$  and  $\tau_{FL}$  for the studied material were calculated to be 316 and 288 MPa, respectively; therefore, the predicted angle was  $\theta = 17^\circ$ .

Models based on a critical plane are widely used in multiaxial fatigue studies. Those of Matake [6] and McDiarmid [7] are especially useful at large numbers of cycles. According to these authors, the critical plane coincides with the direction of the maximum tangential stress (i.e., with  $\theta = 45^\circ$ ). Carpinteri and Spagnoli [8] proposed the following equation to determine the crack initiation direction:

$$\theta = 45 \frac{3}{2} \left( 1 - \left( \frac{\tau_{FL}}{\sigma_{FL}} \right)^2 \right) \tag{2}$$

application of which to the studied material yielded  $\theta = 11^\circ$ .

Tab. 1 shows the experimental and predicted crack directions in the Stage I, expressed in absolute values of  $\alpha$  (i.e., the angle with the  $X$  axis). The models used here allowed  $\alpha$  to be easily calculated from  $\theta$  and the specific type of load applied to the material. Only the results for tests spanning more than  $10^5$  cycles were considered, however, in order to ensure applicability of the hypothesis of models for large numbers of cycles. As can be seen from Tab. 1, the experimental angles were close to  $\alpha = 0^\circ$  in axial tests and increased with increasing torsional loading to a level near  $\alpha = 45^\circ$  in purely torsional tests. The best predictions were obtained with the model of Carpinteri and Spagnoli, followed by that of Chaves et al. On the other hand, the models of Matake and McDiarmid gave much less accurate predictions. In fact, the experimental crack direction at the initiation stage was very close to the normal to the maximum principal stress I (i.e., to that of Mode I). Similar results in this respect were recently obtained by Anes et al. [9] for 42CrMo4 steel and AZ31 magnesium alloy.

Fig. 9 shows the crack direction at Stage I in relation to the normal to the first principal stress, that is,  $\theta$ , for all tests and the predictions of the models. The 20 experimental values of  $\theta$  have been placed consecutively in this graph, in the same order as in Tab. 1. An angle of  $\theta = 0^\circ$  corresponds to a Mode I direction in Stage I, and one of  $45^\circ$  to a Mode II direction. The average experimental angle ( $\theta = 3.5^\circ$ ) was very close to  $0^\circ$  (i.e., it corresponded to Mode I). The predicted angle obtained with the model of Carpinteri and Spagnoli,  $\theta = 11.1^\circ$ , was not very far. However, that obtained with the model of Chaves et al. ( $\theta = 17.0^\circ$ ) was somewhat more dissimilar, and that provided by the model of Matake and McDiarmid ( $\theta = 45.0^\circ$ ) departed even further. In fact, the best prediction of crack direction at Stage I was seemingly that corresponding to Mode I.

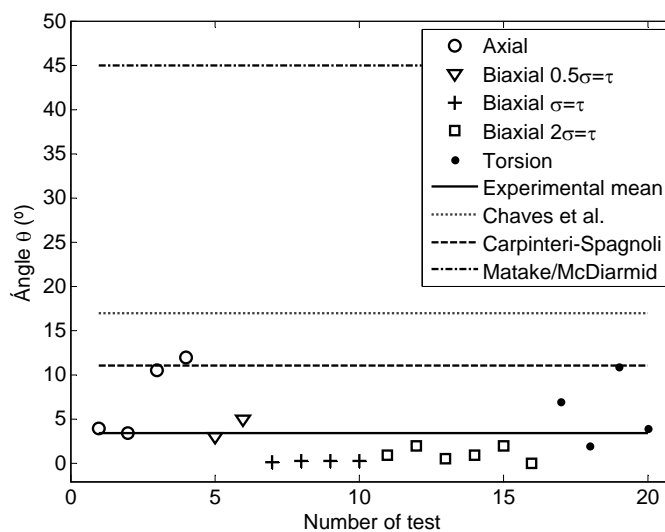


Figure 9: Angle  $\theta$  for the Stage I obtained experimentally and predicted with some models for AISI 304L.



Test	Cycles	Stage I direction, $\alpha$ (°)			
		Experimental	Chaves	Matake	Carpinteri
Axial	119185	4.0	17.0	45.0	11.1
	248683	3.5	17.0	45.0	11.1
	116413	10.5	17.0	45.0	11.1
	145850	12.0	17.0	45.0	11.1
Biaxial	490262	19.5	5.5	22.5	11.4
$0.5\sigma = \tau$	230944	17.5	5.5	22.5	11.4
Biaxial $\sigma = \tau$	424304	31.5	14.7	13.3	20.6
	140828	32.0	14.7	13.3	20.6
	254124	32.0	14.7	13.3	20.6
	204955	32.0	14.7	13.3	20.6
Biaxial $2\sigma = \tau$	460657	37.0	21.0	7.0	26.9
	460663	40.0	21.0	7.0	26.9
	376298	38.5	21.0	7.0	26.9
	398576	37.0	21.0	7.0	26.9
	278760	36.0	21.0	7.0	26.9
	259028	38.0	21.0	7.0	26.9
Torsion	337940	38.0	28.0	0.0	33.9
	623200	43.0	28.0	0.0	33.9
	134300	34.0	28.0	0.0	33.9
	332011	41.0	28.0	0.0	33.9

Table 1: Experimental and predicted Stage I crack directions for AISI 304L steel. In-phase tests ( $R=-1$ )

## SUMMARY AND CONCLUSIONS

AISI 304L stainless steel cylindrical specimens were subjected to biaxial loading fatigue tests in order to construct the  $S-N$  curves for the material. The in-phase biaxial loading curve was better fitted by an elliptical quadrant than by an elliptical arc. Photographs of the cracks on the outer surface of broken specimens taken with a light microscope were used to measure the angle at the crack initiation zone (Stage I), which was found to be close to the direction of Mode I. A comparison of the measured angle with predicted values obtained by using the models of Chaves et al., Matake and McDiarmid, and Carpinteri and Spagnoli, revealed that the last provided the best results in this respect.

## ACKNOWLEDGEMENTS

The authors would like to thank the Spanish Ministry of Education for its financial support through grant DPI2011-27019.



## REFERENCES

- [1] ASTM International, Standard practice for statistical analysis of linear or linearized Stress-life (S-N) and Strain-life (E-N) fatigue data, (2004).
- [2] Bettinelli, S., Sviluppo di metodologie innovative per l'analisi della resistenza a fatica dei materiali e dei componenti meccanici, Tesi di Laurea, Università degli studi di Padova, Supervisor: Prof. Roberto Tovo, (2006).
- [3] Gough, H.J., Pollard, H.V., Clenshaw, W.J., Some Experiments on the Resistance of Metals to Fatigue under Combined Stresses, Ministry of Supply, Aeronautical Research Council Reports and Memoranda, London: His Majesty's Stationary Office, (1951).
- [4] Chaves, V., Navarro, A., Madrigal, C., Vallellano, C., Calculating crack initiation directions for in-phase biaxial fatigue loading, *Int J Fatigue*, 58 (2014) 166-171.
- [5] Navarro, A., Vallellano, C., Chaves, V., Madrigal, C., A microstructural model for biaxial fatigue conditions, *Int J Fatigue*, 33 (2011) 1048-54.
- [6] Mataka, T., An explanation on fatigue limit under combined stress, *Bull JSME* 20 (1977) 257-63.
- [7] McDiarmid, D.L., A general criterion for high cycle multiaxial fatigue failure, *Fatigue Fract Engng Mater Struct*, 14 (1991) 429-53.
- [8] Carpinteri, A., Spagnoli, A., Multiaxial high-cycle fatigue criterion for hard metals, *Int J Fatigue*, 23 (2001) 135-145.
- [9] Anes, V., Reis, L., Li, B., Freitas, M., Crack path evaluation on HC and BCC microstructures under multiaxial cyclic loading, *Int J Fatigue*, 58 (2014) 102-113.